

| REPORT DOCUMENTATION PAGE   |             |                            | Form Approved OMB NO. 0704-0188                       |                                 |  |
|---|-------------|----------------------------|---|---------------------------------|--|
| <p>The public reporting burden for this collection of information is estimated to average 1 hour per response, including the time for reviewing instructions, searching existing data sources, gathering and maintaining the data needed, and completing and reviewing the collection of information. Send comments regarding this burden estimate or any other aspect of this collection of information, including suggestions for reducing this burden, to Washington Headquarters Services, Directorate for Information Operations and Reports, 1215 Jefferson Davis Highway, Suite 1204, Arlington VA, 22202-4302. Respondents should be aware that notwithstanding any other provision of law, no person shall be subject to any penalty for failing to comply with a collection of information if it does not display a currently valid OMB control number.</p> <p>PLEASE DO NOT RETURN YOUR FORM TO THE ABOVE ADDRESS.</p> |             |                            |   |                                 |  |
| 1. REPORT DATE (DD-MM-YYYY)   |             | 2. REPORT TYPE             |   | 3. DATES COVERED (From - To)    |  |
|   |             | New Reprint                |   | -                               |  |
| 4. TITLE AND SUBTITLE<br>Photothermally Activated Motion and Ignition Using Aluminum Nanoparticles  |             |                            | 5a. CONTRACT NUMBER                                   |                                 |  |
|   |             |                            | W911NF-10-1-0114                                      |                                 |  |
|   |             |                            | 5b. GRANT NUMBER                                      |                                 |  |
|   |             |                            | 5c. PROGRAM ELEMENT NUMBER                            |                                 |  |
|   |             |                            | 611102  |                                 |  |
| 6. AUTHORS<br>Jacques E. Abboud, Xinyuan Chong, Mingjun Zhang, Zhili Zhang, Naibo Jiang, Sukesh Roy, James R. Gord  |             |                            | 5d. PROJECT NUMBER                                    |                                 |  |
|   |             |                            | 5e. TASK NUMBER                                       |                                 |  |
|   |             |                            | 5f. WORK UNIT NUMBER                                  |                                 |  |
| 7. PERFORMING ORGANIZATION NAMES AND ADDRESSES  |             |                            | 8. PERFORMING ORGANIZATION REPORT NUMBER              |                                 |  |
| University of Tennessee at Knoxville<br>Office of Research<br>The University of Tennessee<br>Knoxville, TN 37996 -1529  |             |                            |   |                                 |  |
| 9. SPONSORING/MONITORING AGENCY NAME(S) AND ADDRESS(ES)<br>U.S. Army Research Office<br>P.O. Box 12211<br>Research Triangle Park, NC 27709-2211   |             |                            | 10. SPONSOR/MONITOR'S ACRONYM(S)<br>ARO               |                                 |  |
|   |             |                            | 11. SPONSOR/MONITOR'S REPORT NUMBER(S)<br>56015-LS.23 |                                 |  |
| 12. DISTRIBUTION AVAILABILITY STATEMENT<br>Approved for public release; distribution is unlimited.  |             |                            |   |                                 |  |
| 13. SUPPLEMENTARY NOTES<br>The views, opinions and/or findings contained in this report are those of the author(s) and should not be construed as an official Department of the Army position, policy or decision, unless so designated by other documentation.   |             |                            |   |                                 |  |
| 14. ABSTRACT<br>The aluminum nanoparticles (Al NPs) are demonstrated to serve as active photothermal media, to enhance and control local photothermal energy deposition via the photothermal effect activated by localized surface plasmon resonance (LSPR) and amplified by Al NPs oxidation. The activation source is a 2-AA-battery-powered xenon flash lamp. The extent of the photothermally activated movement of Al NPs can be $\square$ 6 mm. Ignition delay can be $\square$ 0.1 ms. Both scanning electron  |             |                            |   |                                 |  |
| 15. SUBJECT TERMS<br>Nanoparticles, aluminum nanoparticles, photothermally activation   |             |                            |   |                                 |  |
| 16. SECURITY CLASSIFICATION OF:   |             | 17. LIMITATION OF ABSTRACT |   | 15. NUMBER OF PAGES             |  |
| a. REPORT   | b. ABSTRACT | c. THIS PAGE               | UU  | 19a. NAME OF RESPONSIBLE PERSON |  |
| UU  | UU          | UU                         |   | Mingjun Zhang                   |  |
|   |             |                            |   | 19b. TELEPHONE NUMBER           |  |
|   |             |                            |   | 865-974-7620                    |  |

## Report Title

Photothermally Activated Motion and Ignition Using Aluminum Nanoparticles

### ABSTRACT

The aluminum nanoparticles (Al NPs) are demonstrated to serve as active photothermal media, to enhance and control local photothermal energy deposition via the photothermal effect activated by localized surface plasmon resonance (LSPR) and amplified by Al NPs oxidation. The activation source is a 2-AA-battery-powered xenon flash lamp. The extent of the photothermally activated movement of Al NPs can be  $\approx 6$  mm. Ignition delay can be  $\approx 0.1$  ms. Both scanning electron microscopy and energy-dispersive X-ray spectroscopy measurements of motion-only and afterignition products confirm significant Al oxidation occurs through sintering and bursting after the flash exposure. Simulations suggest local heat generation is enhanced by LSPR. The positive feedback effects from the local heat generation amplified by Al oxidation produce a large increase in local temperature and pressure, which enhances movement and accelerates ignition.

---

**REPORT DOCUMENTATION PAGE (SF298)**  
**(Continuation Sheet)**

---

Continuation for Block 13

ARO Report Number 56015.23-LS  
Photothermally Activated Motion and Ignition Us ...

Block 13: Supplementary Note

© 2013 . Published in Applied Physics letters, Vol. Ed. 0 102, (23905) (2013), (3905). DoD Components reserve a royalty-free, nonexclusive and irrevocable right to reproduce, publish, or otherwise use the work for Federal purposes, and to authorize others to do so (DODGARS §32.36). The views, opinions and/or findings contained in this report are those of the author(s) and should not be construed as an official Department of the Army position, policy or decision, unless so designated by other documentation.

Approved for public release; distribution is unlimited.

## Photothermally activated motion and ignition using aluminum nanoparticles

Jacques E. Abboud, Xinyuan Chong, Mingjun Zhang, Zhili Zhang, Naibo Jiang et al.

Citation: *Appl. Phys. Lett.* **102**, 023905 (2013); doi: 10.1063/1.4776660

View online: <http://dx.doi.org/10.1063/1.4776660>

View Table of Contents: <http://apl.aip.org/resource/1/APPLAB/v102/i2>

Published by the [American Institute of Physics](#).

### Related Articles

Photothermal model fitting in the complex plane for thermal properties determination in solids  
*Rev. Sci. Instrum.* **84**, 024903 (2013)

Improvement of the identification of multiwall carbon nanotubes carpet thermal conductivity by pulsed photothermal method  
*J. Appl. Phys.* **112**, 094322 (2012)

Photothermal characterization of the thermal properties of materials using four characteristic modulation frequencies in two-layer systems  
*J. Appl. Phys.* **112**, 064909 (2012)

Propagation of thermal waves across a wedge  
*J. Appl. Phys.* **112**, 063511 (2012)

Laser induced thermal-wave fields in multi-layered spherical solids based on Green function method  
*J. Appl. Phys.* **112**, 033521 (2012)

### Additional information on *Appl. Phys. Lett.*

Journal Homepage: <http://apl.aip.org/>

Journal Information: [http://apl.aip.org/about/about\\_the\\_journal](http://apl.aip.org/about/about_the_journal)

Top downloads: [http://apl.aip.org/features/most\\_downloaded](http://apl.aip.org/features/most_downloaded)

Information for Authors: <http://apl.aip.org/authors>

## ADVERTISEMENT

**AIP** | Applied Physics  
Letters

**SURFACES AND INTERFACES**  
Focusing on physical, chemical, biological, structural, optical, magnetic and electrical properties of surfaces and interfaces, and more...

**ENERGY CONVERSION AND STORAGE**  
Focusing on all aspects of static and dynamic energy conversion, energy storage, photovoltaics, solar fuels, batteries, capacitors, thermoelectrics, and more...

**EXPLORE WHAT'S NEW IN APL**

**SUBMIT YOUR PAPER NOW!**

## Photothermally activated motion and ignition using aluminum nanoparticles

Jacques E. Abboud,<sup>1</sup> Xinyuan Chong,<sup>1</sup> Mingjun Zhang,<sup>1</sup> Zhili Zhang,<sup>1,a)</sup> Naibo Jiang,<sup>2</sup> Suresh Roy,<sup>2</sup> and James R. Gord<sup>3</sup>

<sup>1</sup>Mechanical, Aerospace and Biomedical Engineering Department, University of Tennessee, Knoxville, Tennessee 37996, USA

<sup>2</sup>Spectral Energies, LLC, 5100 Springfield Street, Suite 301, Dayton, Ohio 45431, USA

<sup>3</sup>Air Force Research Laboratory, Propulsion Directorate, Wright-Patterson Air Force Base, Ohio 45433, USA

(Received 15 August 2012; accepted 27 December 2012; published online 17 January 2013)

The aluminum nanoparticles (Al NPs) are demonstrated to serve as active photothermal media, to enhance and control local photothermal energy deposition via the photothermal effect activated by localized surface plasmon resonance (LSPR) and amplified by Al NPs oxidation. The activation source is a 2-AA-battery-powered xenon flash lamp. The extent of the photothermally activated movement of Al NPs can be  $\sim 6$  mm. Ignition delay can be  $\sim 0.1$  ms. Both scanning electron microscopy and energy-dispersive X-ray spectroscopy measurements of motion-only and after-ignition products confirm significant Al oxidation occurs through sintering and bursting after the flash exposure. Simulations suggest local heat generation is enhanced by LSPR. The positive-feedback effects from the local heat generation amplified by Al oxidation produce a large increase in local temperature and pressure, which enhances movement and accelerates ignition. © 2013 American Institute of Physics. [<http://dx.doi.org/10.1063/1.4776660>]

Efficient control of local photothermal energy deposition at the nanoscale has numerous impacts on nanotechnology, including nanoscale detection,<sup>1–3</sup> photothermal tumor therapy,<sup>2,4,5</sup> nanorotors,<sup>6</sup> and thermoelectric solar cells.<sup>7–9</sup> However, most of the current research can be categorized as “passive,”<sup>10,11</sup> being focused on the unique nanostructures of the noble metals and specific light wavelength/duration/power to induce thermal effects. The underlying physics is localized surface plasmon resonance (LSPR), which utilize resonant oscillation of free electrons in the metals under light illumination to confine, enhance, localize, or guide light radiations in the nanoscale structures. In searching better media for LSPR enhanced photothermal energy deposition, aluminum is less attractive compared to the noble metals.<sup>3,12,13</sup> Aluminum has significantly more thermal ohmic losses than the noble metals in the ultraviolet (UV) and visible ranges due to larger dielectric constants in those regions.<sup>14</sup> Additionally, pure aluminum is easily oxidized in the atmospheric environments.

In recent years, nanoenergetic materials have been extensively studied because of their high-energy densities and fast reaction rates.<sup>15</sup> Some research on flash ignition of single-wall carbon nanotubes (SWCNT) and aluminum nanoparticles (Al NPs) has been reported in the literature.<sup>16–18</sup> In comparison with alternative sources such as spark ignition,<sup>19</sup> laser ignition,<sup>20</sup> plasma ignition,<sup>21</sup> plasma-assisted combustion,<sup>22</sup> and combustion enhancement through the use of catalytic nanomaterials,<sup>23</sup> flash ignition has many benefits because of its lower power, lower material cost, lower mass, and no quenching from electrode-less configuration. SWCNT with metal impurities have been demonstrated to provide precise control over the time and location of a chemical reaction,<sup>24</sup> which may enable more rapid and homogeneous ignition and combustion, enhance flame speed, and stabilize burning at extremely lean

conditions (fuel/air ratio significantly less than stoichiometric, leading to ultralow emissions).

Here, we report an active approach for controlling the photothermal effect of the Al NPs by engaging local oxidation reactions, which has the potential to open another avenue for innovations in applications in combustion, propulsion, solar cells, and photothermal tumor therapy. The overall process is similar to positive feedback, which is much more efficient than “passive” laser-induced photothermal ejection.<sup>25,26</sup> The photothermal effect is initiated and controlled by a xenon flash lamp that is powered by two AA batteries. LSPR effects confine and enhance the optical energy within the nanoenergetic particles. The oxidation reactions of the nanoenergetic particles are, thus, activated by the local temperature increase and provide additional energy that is sufficient to accelerate the chemical reactions. As a comparison, “passive” photothermal effect is to couple the light energy in the aluminum nanostructures and prevent the oxidation reactions.<sup>27–29</sup> Since the chemical energy from the nanoenergetics is much higher and more efficient than the photothermal activation energy, the active photothermal approach is to control local energy deposition with a light trigger.

*Setup:* A commercial xenon flash was used as the photothermal source in our experiments. The average diameter of the Al NPs (NanoAmor Inc.) used was  $\sim 70$  nm. To control the input energy from the flash, the NPs were placed on a glass slide at various distances from the end surface of the flash. The flash power was measured by a long-pulse-thermopile power sensor. The power decreased roughly linear with respect to distance.<sup>30</sup> The maximum power used in the experiment was  $1.9 \text{ J/cm}^2$ , which corresponded to a distance of 1 cm between the NPs and the end surface of the flash source. Sending the flash through a long-pass filter with a cutoff wavelength at 540 nm decreased the total power by  $\sim 25\%$ . Since UV light  $< 350$  nm was blocked by the BK7/glass cover of the flash, the spectral profile of the flash

<sup>a)</sup>Email: zzhang24@utk.edu.

covered from 350 nm to the deep-infrared range. The flash had a temporal profile including a spike of  $\sim 50 \mu\text{s}$ , a plateau of  $\sim 6 \text{ ms}$ , and a decay of 5 ms at full power. At different power levels, the duration of the plateau and decay portions changed, but the spike remained similar. The spectra of the flash remained similar for different portions of the spike, plateau, and decay at different power levels.

**Motion:** The photothermally activated motion of Al NPs was observed with a fast camera (Photron Company FAST-CAM SA5). Figure 1(a) (Ref. 30) shows the temporally resolved images of the motion activated by the flash, corresponding to different portions of the flash. The first image shows the non-impacted Al NP pile. The frames within the first 10 ms were saturated by the flash, which are not shown in Figure 1(a). The NPs began to move upward in the early stage of the flash pulse. A large portion of the nanoparticle pile was driven away from the surface. The highest point reached up to 6 mm from the surface without ignition is shown in the ninth image. The movement is  $\sim 10^5$  times higher than that from femtosecond/nanosecond laser-induced photothermal ejection of gold nanodroplets.<sup>25,26</sup>

Two important features for the photothermally activated motion have been identified. First, the delay between the incidence of the light and the motion is on the order of tens of microseconds. Additionally, the Al NP motion can be controlled by varying the magnitude of the energy input and/or UV light filtering, as shown in Figure 1(b). A decrease in the flash power can lead to a decrease in the height of the motion. When a long-pass filter with the cutoff wavelength at 540 nm was placed between the NPs and the flash, a decrease in the height of the motion was also observed.

Second, the NPs can be moved up by the flash-activation oxidation without ignition, which has been confirmed by scanning electron microscopy (SEM) and energy-dispersive X-ray spectroscopy (EDS) analyses. The original Al NPs are uniform in size, with ellipsoidal and irregular shapes.<sup>30</sup> Aggregation of multiple NPs can be observed. After the flash exposure, two types of products—larger particles with diameters of several microns and smaller NPs with diameters of  $\sim 50 \text{ nm}$ —have been found in the Al NP residues. Large particles were formed through sintering multiple Al NPs. Smaller NPs were formed through bursting. EDS analyses show that the original Al NPs are slightly and non-uniformly oxidized. The mole ratio of Al to oxygen is about 4:1, varying slightly for different locations

inside the NP pile because of local oxidation. After a single exposure of the flash, the Al NPs become more uniformly oxidized. The mole ratios decrease to  $\sim 2.5:1$  for the melted Al NPs and to 1.4:1 for the burst ones. A significant amount of the oxidation occurs after the flash exposure, even without ignition.

**Ignition:** When the flash power was increased, flash-activated ignition of Al NPs was experimentally observed shown in Figure 2. Al NPs at the periphery of the pile were ignited first. The combustion propagated toward the center and the bottom of the sample. A sample of 10 mg of Al NPs ignited in air has an average combustion time of  $\sim 10 \text{ s}$ . Al NPs can be consecutively ignited up to four times, with an average combustion duration of  $\sim 7 \text{ s}$  for each ignition. The total combustion process can last more than 30 s. The ignition delay was recorded by a high-speed camera operated at 100 kHz. For Al NPs with an average diameter of  $\sim 70 \text{ nm}$ , the ignition delay was  $\sim 0.12 \text{ ms}$  with the flash, as shown in Figure 2, which is about 100 times faster than that by conductive heating.<sup>31</sup> The ignition process is highly localized. Similarly, the entire Al NP pile has been lifted about 1 mm above the surface by the photothermal activation.

UV light filtering has been used to control the ignition of the Al NPs. Long-pass filtering with the cutoff wavelength at 540 nm leads to a decrease in height, and ignition may not be triggered under the illumination of the flash at certain powers with filtering. For a flash power of  $1.1 \text{ J/cm}^2$  with filtering, which corresponds to 1.6 cm from the flash end surface, ignition is not induced. At a similar power level without filtering, i.e., power without filtering at 2.5 cm, the Al NPs can be ignited. Further increase of the flash power with filtering to  $\sim 1.3 \text{ J/cm}^2$  can induce ignition, as shown in Figure 2(b). This indicates higher efficiency of UV light for ignition. Ignition can be achieved for a pile of  $< 0.5 \text{ mg}$ . SEM images of Al NPs after the flash ignition and burning are shown in Ref. 30. Similar to the movement without ignition, the Al NPs either melt into larger particles or burst into smaller NPs. As a comparison, EDS analyses of the product at the burning regions show that the mole ratio of Al to oxygen is  $\sim 1:2$ , indicating that more than 80% of the Al has been oxidized to alumina.

**Simulations and suggested mechanisms:** The effect of the direct absorption-induced global heating has been determined. Light absorption using the discrete dipole approximation (DDA)<sup>32</sup> for alumina-coated NPs with various shapes,

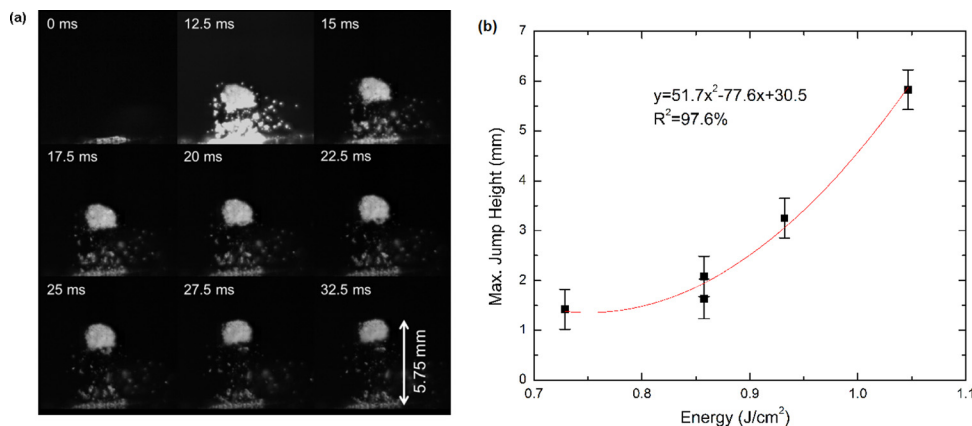


FIG. 1. Photothermally activated motion of Al NPs with a single xenon flash pulse. (a) Photothermally activated motion of NPs observed by a fast camera at a frame rate of 10 kHz. Each frame size is 8.6 mm in height  $\times$  8.9 mm in width. (b) Height of photothermally activated motion is approximately quadratically dependent of flash power (enhanced online) [URL: <http://dx.doi.org/10.1063/1.4776660.1>].

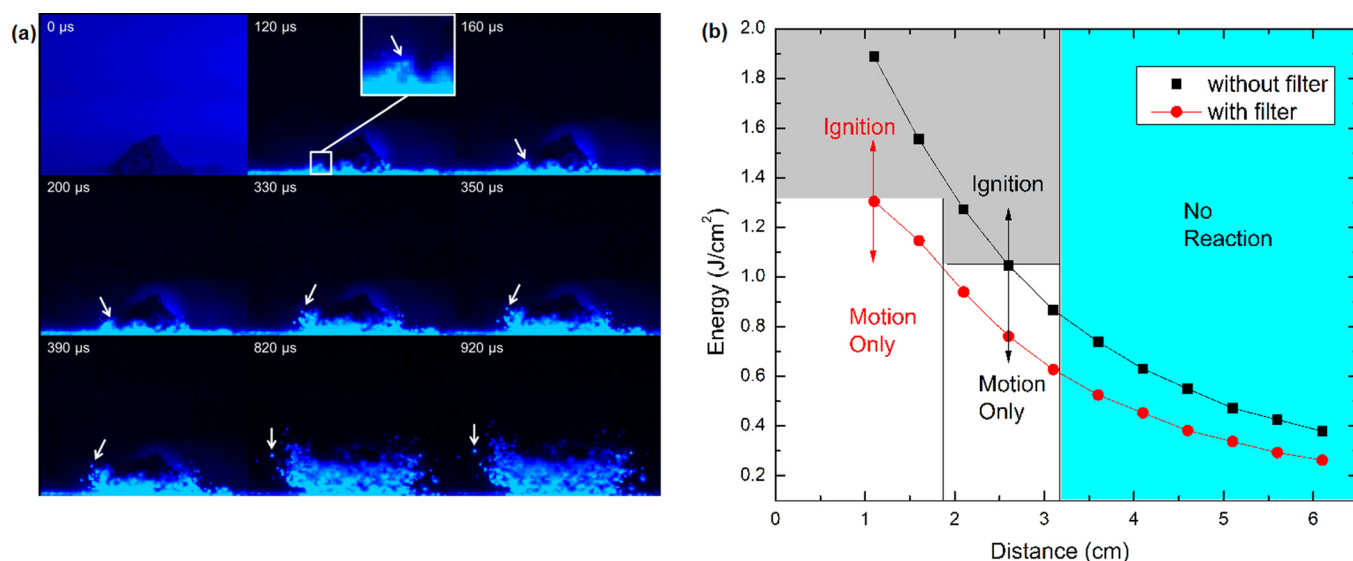


FIG. 2. (a) Photothermally driven ignition of Al NPs by a single xenon flash pulse at a frame rate of 100 kHz, at incident power of  $1.6 \text{ J}/\text{cm}^2$ . Ignition was identified in the second image, which was acquired  $\sim 0.12 \text{ ms}$  after the flash incidence. Ignition is spatially localized. Each frame size is  $3.8 \text{ mm}$  in height  $\times$   $4.9 \text{ mm}$  in width. (b) Flash power dependence for transition of ignition and motion only with and without the long pass filter cutoff at  $540 \text{ nm}$ . It shows that UV is more efficient for motion and ignition (enhanced online) [URL: <http://dx.doi.org/10.1063/1.4776660.2>].

sizes, coating thicknesses, and aggregation configurations was computed. In DDA, each particle is represented by an array of point dipoles. The absorption behavior of the target was calculated, based on the interactions between the incident light and the dipoles. The absorption spectra for several configurations of the experiment are given in Ref. 30. The peak wavelengths of the plasmon resonance of the Al NPs shift from  $\sim 200 \text{ nm}$  for spherical particles to the visible and near-infrared regions for prolonged spheres. To take into account the aggregation effects, absorption by multiple Al NPs was calculated. Similar red shifts were observed. The plasmon resonance and absorption occurred mainly within the near UV and visible range for these configurations.

It has been confirmed through simulation that the global heating of Al NPs by absorption of the flash light is not the main contributor for the ignition of a single Al NP. It should be noted that there is no consensus in the open literature on

thermal ignition of metal nanoenergetic materials. For Al NPs, the reported ignition temperature ranges from  $900 \text{ K}$  (below the Al melting point) to  $2300 \text{ K}$  (close to the melting point of alumina).<sup>15,31,33</sup> The global-temperature increase of a single Al NP due to light absorption was calculated using the standard heat-transfer equation.<sup>11,34–36</sup> The heat generated by the light absorption was obtained by integration of the flash spectrum over the theoretical absorption curve. The total temperature increase for a single Al NP is  $< 1 \text{ K}$  for the input power of  $2 \text{ J}/\text{cm}^2$ . This result suggests that certain kinetic or local heating effects in addition to global heating have contributed to the flash-activated motion and ignition of the Al NPs.

Positive feedback, initiated by plasmon-resonance-enhanced local heating and further amplified by the Al oxidation reaction, is suggested to be responsible for sintering the Al NPs<sup>31,37</sup> and rupture of the alumina shell.<sup>33,38</sup> Figure 3

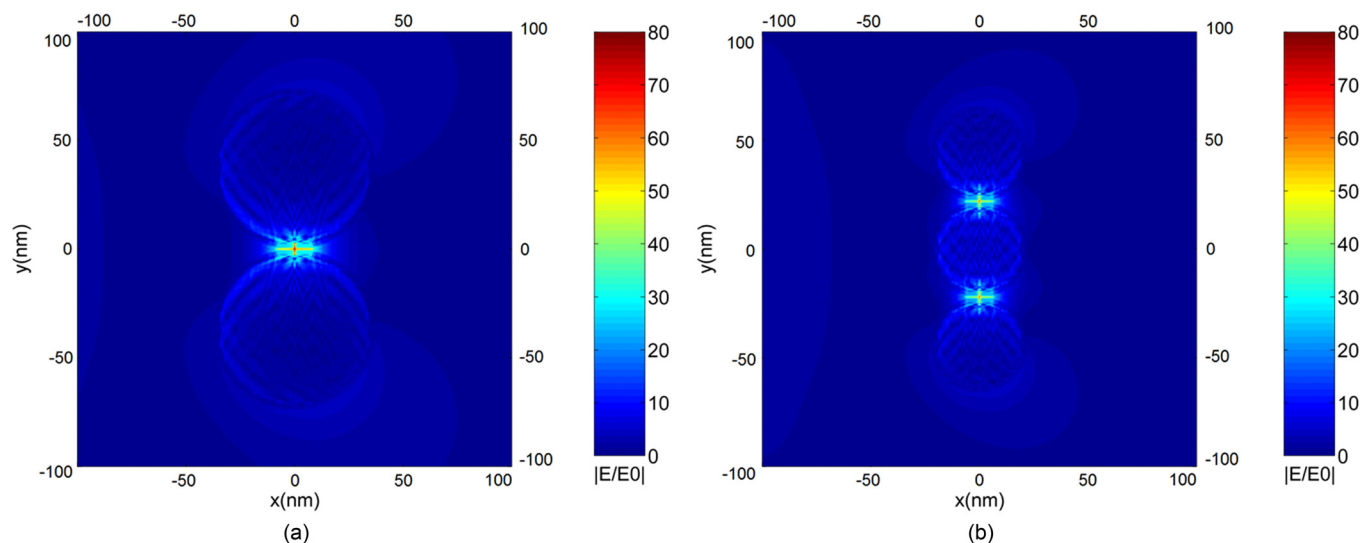


FIG. 3. Electric-field distributions under the flash illumination for NPs with 2-nm alumina shell and aluminum core at their plasmon resonance. (a) Two contacting spheres with radii of  $35 \text{ nm}$ . The plasmon resonance is at  $381 \text{ nm}$ . (b) Three contacting spheres with radii of  $20 \text{ nm}$ . The plasmon resonance is at  $354 \text{ nm}$ . For both cases, the local electric-field enhancement can reach as much as 80 times, leading to local heat enhancement up to 6400 times as compared to the global heating.

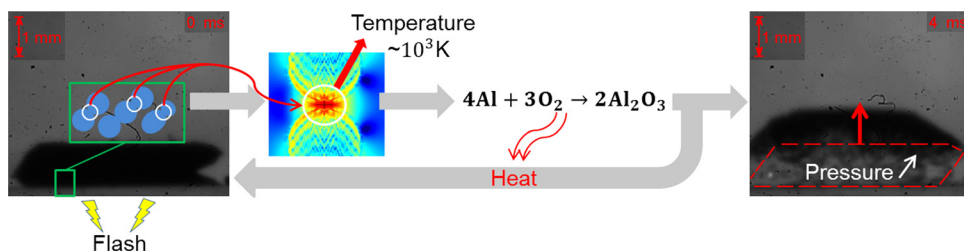


FIG. 4. Suggested positive feedback mechanism for the flash-induced photothermally activated motion and ignition of Al NPs.

shows the distribution of the local electric field near the Al NPs with 2-nm-thick alumina coating at various wavelengths. In the calculation, the electromagnetic wave was propagating from left to right. The local fields were clearly enhanced near the interface between the alumina shell and the Al core. The location of the enhancement depends on the wavelength of the incident light and the relative positions of multiple NPs. In the near UV-region, the electric-field enhancement inside a single spherical Al NP is less than five times that of the original incident electric field, while the maximum enhancement in the two contacting spherical NPs at the plasmonic resonance is  $\sim 80$ , as shown in Figure 3. Since the local heat flux is  $\Delta Q = 1/2\epsilon_0\omega\text{Im}(\epsilon_r)|E|^2$ , where  $\epsilon_0$  is the permittivity of the vacuum,  $\epsilon_r$  is the relative permittivity of Al or alumina,  $\omega$  is the frequency of the light, and  $E$  is the electric field, the local heat generation can be enhanced up to 6400 times, leading to a large increase in the local temperature and thus pressure. For a 5-nm region near the largest enhancement in the Al NPs, the local temperature can reach  $\sim 1070$  K, which is sufficiently high to activate the local oxidation process. This is consistent with the results of EDS analyses of Al NPs after the pure movement and ignition. Positive-feedback processes of local heating generation and Al oxidation also move and/or ignite the Al NPs. For the small gaps in the Al NPs pile, the pressure may increase four to eight times as a result of the rapid temperature rise. Thus, the force applied to the Al NPs pushes them upward.

Figure 4 shows the overall suggested mechanism of the photothermally activated process. The plasmon resonance among Al NPs generates a significant amount of local heat. The oxidation reactions of Al are, thus, activated. Through positive feedback, a significant increase in the local temperature and pressure is produced, which results in the motion and ignition of Al NPs. Since the Al NPs used in the experiments are spherical and slightly oblate, as shown in the SEM images, the plasmon resonance occurs mainly at the near-UV and visible ranges. Thus, light in the near-UV range is more efficient for ignition, in agreement with our experimental observations.

We reported the properties of Al NPs as an active photo-thermal media to enhance and control local heat generation, particle motion, and ignition via LSPR and Al oxidation. The photothermally activated movement of NPs under a single 10 ms pulse from a xenon flash can be as high as 6 mm from the surface without ignition, which is  $\sim 10^5$  times higher than that from femtosecond/nanosecond laser-induced photothermal ejection of gold nanodroplets. Depending on the flash power and spectrum, ignition delay by the flash can be on the order of 0.1 ms, which is  $\sim 100$  times faster than ignition by conductive heating. Active control by varying the flash power or UV filtering of the low power xenon flash has

been achieved for both motion and ignition. Both SEM and EDS measurements of motion-only and after-ignition products indicate significant oxidation of Al NPs occurs through sintering and bursting after a single flash exposure. Electromagnetic simulations indicate that the local heat generation is significantly enhanced by the local electric field inside and among the alumina-coated Al NPs. The positive feedback effects from the local heat generation are amplified by Al oxidation. The local heat-induced pressure pulse in the NPs is responsible for the large movement. The local heating inside and among the NPs generates and accelerates the ignition.

We acknowledge the encouragement and support from AFOSR program manager Dr. Chiping Li for this work. The work at the University of Tennessee Knoxville was supported by NSF CBET-1032523 and ARO W911NF-10-1-0114. Funding for Spectral Energies is provided by the Air Force Research Laboratory under Contract No. FA8650-10-C-2008.

- <sup>1</sup>D. Boyer, P. Tamarat, A. Maali, B. Lounis, and M. Orrit, *Science* **297**, 1160–1163 (2002).
- <sup>2</sup>A. M. Gobin, M. H. Lee, N. J. Halas, W. D. James, R. A. Drezek, and J. L. West, *Nano Lett.* **7**, 1929–1934 (2007).
- <sup>3</sup>G. H. Chan, J. Zhao, G. C. Schatz, and R. P. V. Duyne, *J. Phys. Chem. C* **112**, 13958–13963 (2008).
- <sup>4</sup>E. Y. Lukianova-Hleb, X. Ren, J. A. Zasadzinski, X. Wu, and D. O. Lapotko, *Adv. Mater.* **24**, 3831–3837 (2012).
- <sup>5</sup>E. Y. Lukianova-Hleb, A. Belyanin, S. Kashinath, X. Wu, and D. O. Lapotko, *Biomaterials* **33**, 1821–1826 (2012).
- <sup>6</sup>A. M. Fennimore, T. D. Yuzvinsky, W.-Q. Han, M. S. Fuhrer, J. Cumings, and A. Zettl, *Nature* **424**, 408–410 (2003).
- <sup>7</sup>M. Tursunov, R. Muminov, O. Tukfatullin, I. Yuldoshev, and E. Abdullaev, *Appl. Sol. Energy* **47**, 63–65 (2011).
- <sup>8</sup>S. Linic, P. Christopher, and D. B. Ingram, *Nature Mater.* **10**, 911–921 (2011).
- <sup>9</sup>C. Hägglund and S. P. Apell, *J. Phys. Chem. Lett.* **3**, 1275–1285 (2012).
- <sup>10</sup>S. Link and M. A. El-Sayed, *Int. Rev. Phys. Chem.* **19**, 409–453 (2000).
- <sup>11</sup>A. O. Govorov and H. H. Richardson, *Nano Today* **2**, 30–38 (2007).
- <sup>12</sup>P. R. West, S. Ishii, G. V. Naik, N. K. Emani, V. M. Shalaev, and A. Boltasseva, *Laser Photon. Rev.* **4**, 795–808 (2010).
- <sup>13</sup>D. W. Hammerstroem, M. A. Burgers, S. W. Chung, E. A. Gulians, C. E. Bunker, K. M. Wentz, S. E. Hayes, S. W. Buckner, and P. A. Jelliss, *Inorg. Chem.* **50**, 5054–5059 (2011).
- <sup>14</sup>*Handbook of Optical Constants of Solids*, edited by E. D. Palik (Academic, San Diego, 1998).
- <sup>15</sup>E. L. Dreizin, *Prog. Energy Combust. Sci.* **35**, 141–167 (2009).
- <sup>16</sup>D. J. Finigan, B. D. Dohm, J. A. Mockelman, and M. A. Oehlschlaeger, *Combust. Flame* **159**, 1314–1320 (2012).
- <sup>17</sup>P. M. Ajayan, M. Terrones, A. de la Guardia, V. Huc, N. Grobert, B. Q. Wei, H. Lezec, G. Ramanath, and T. W. Ebbesen, *Science* **296**, 705 (2002).
- <sup>18</sup>Y. Ohkura, P. M. Rao, and X. Zheng, *Combust. Flame* **158**, 2544–2548 (2011).
- <sup>19</sup>G. Lacaze, E. Richardson, and T. Poinsot, *Combust. Flame* **156**, 1993–2009 (2009).
- <sup>20</sup>S. Joshi, D. B. Olsen, C. Dumitrescu, P. V. Puzinauskas, and A. P. Yalin, *Appl. Spectrosc.* **63**, 549–554 (2009).
- <sup>21</sup>C. D. Cathey, T. Tao, T. Shiraiishi, T. Urushihara, A. Kuthi, and M. A. Gundersen, *IEEE Trans. Plasma Sci.* **35**, 1664–1668 (2007).

- <sup>22</sup>S. M. Starikovskaia, *J. Phys. D: Appl. Phys.* **39**, R265 (2006).
- <sup>23</sup>T. Shimizu, A. D. Abid, G. Poskrebshev, H. Wang, J. Nabity, J. Engel, J. Yu, D. Wickham, B. Van Devener, S. L. Anderson, and S. Williams, *Combust. Flame* **157**, 421–435 (2010).
- <sup>24</sup>A. M. Berkowitz and M. A. Oehlschlaeger, *Proc. Combust. Inst.* **33**, 3359–3366 (2011).
- <sup>25</sup>A. Habenicht, M. Olapinski, F. Burmeister, P. Leiderer, and J. Boneberg, *Science* **309**, 2043–2045 (2005).
- <sup>26</sup>M. Fuentes-Cabrera, B. H. Rhodes, M. I. Baskes, H. Terrones, J. D. Fowlkes, M. L. Simpson, and P. D. Rack, *ACS Nano* **5**, 7130–7136 (2011).
- <sup>27</sup>M. W. Knight, L. Liu, Y. Wang, L. Brown, S. Mukherjee, N. S. King, H. O. Everitt, P. Nordlander, and N. J. Halas, *Nano Lett.* **12**, 6000–6004 (2012).
- <sup>28</sup>A. Taguchi, Y. Saito, K. Watanabe, S. Yijian, and S. Kawata, *Appl. Phys. Lett.* **101**, 081110 (2012).
- <sup>29</sup>M. Castro-Lopez, D. Brinks, R. Sapienza, and N. F. van Hulst, *Nano Lett.* **11**, 4674–4678 (2011).
- <sup>30</sup>See supplementary material at <http://dx.doi.org/10.1063/1.4776660> for the height dependence of flash power (Figure S1), SEM images of Al NPs (Figure S2), SEM images of Al NPs after flash ignition and burning (Figure S3), and absorption spectra of various Al NPs (Figure S4).
- <sup>31</sup>R. A. Yetter, G. A. Risha, and S. F. Son, *Proc. Combust. Inst.* **32**, 1819–1838 (2009).
- <sup>32</sup>B. T. Draine and P. J. Flatau, *J. Opt. Soc. Am. A* **11**, 1491–1499 (1994).
- <sup>33</sup>V. I. Levitas, *Combust. Flame* **156**, 543–546 (2009).
- <sup>34</sup>E. Y. Hleb and D. O. Lapotko, *Nanotechnology* **19**, 355702 (2008).
- <sup>35</sup>G. Baffou, C. Girard, and R. Quidant, *Phys. Rev. Lett.* **104**, 136805 (2010).
- <sup>36</sup>G. Baffou, R. Quidant, and C. Girard, *Phys. Rev. B* **82**, 165424 (2010).
- <sup>37</sup>K. T. Sullivan, N. W. Piekiet, C. Wu, S. Chowdhury, S. T. Kelly, T. C. Hufnagel, K. Fezzaa, and M. R. Zachariah, *Combust. Flame* **159**, 2–15 (2012).
- <sup>38</sup>Y. Aly, M. Schoenitz, and E. L. Dreizin, *Combust. Sci. Technol.* **183**, 1107–1132 (2011).